Effect of Hot Deformation on the Wear Behavior of Al_2O_3/ A356 Nano-Composites

Nawal Ezzat Abdul-latiff[1], Akeel Dhahir Subhi[1] & Marwan Basil Hussein[1]

[1] Department of Production Engineering and Metallurgy, University of Technology, Baghdad, Iraq

Correspondence: Akeel Dhahir Subhi, Department of Production Engineering and Metallurgy, University of Technology, Baghdad, Iraq. Tel: 964-780-882-7048. E-mail: drengads@yahoo.com

Abstract

In the present work, Al_2O_3/A356 nano composites with different Al_2O_3 nano sizes (10 and 20 nm) and weight percentages (1 and 2 wt.%) have been prepared using rheocasting technique and followed by hot deformation at 250 $^\circ$C with different ratios (30 and 40%). Pin on disc wear test was used to study wear behavior of prepared Al_2O_3/A356 nano composites while scanning electron microscopy used to build up the wear mechanism. The results showed that the hot deformed nano Al_2O_3 /A356 composites have lower wear rate compared with non deformed one. Furthermore, with increasing the particle size and percentage of Al_2O_3 nano particles, wear rate decreased. The optimal result was achieved at the nano-composite containing 20 nm Al_2O_3 particles after hot deformation with ratio of 40%. SEM studies of the worn surfaces of nano composites showed that the main wear mechanism was oxidative in conjunction with metallic one.

Keywords: A356 alloy, nano composite, hot deformation, wear

1. Introduction

Metal matrix nano composites (MMNCs) are lightweight, high strength materials with potential applications in areas such as automobile, aerospace and military. They significantly reduce the overall weight of vehicles and aircrafts while maintaining satisfactory structural strength. In MMNCs, enhanced mechanical properties of aluminum alloys such as higher tensile strength and longer fatigue life have been achieved by embedding nano-sized ceramic particles (typically less than 100 nm in size) into the metal matrix (Zhou et al., 2012; Saheb et al., 2012).

Semi-solid process as in rheocasting can produce good quality of MMCs. The preparation procedure for rheocast composites consists of the incorporation of the ceramic particles within very vigorously agitated semi-solid alloy slurry which can achieve more homogenous particles distribution as compared with a fully molten alloy (Canyook et al., 2010).

El-Kady et al. (2011) studied the A356/Al_2O_3 nanocomposites fabricated using a combination between the rheocasting and squeeze casting techniques. They showed that the A356/Al_2O_3 nanocomposites exhibited better mechanical properties than the A356 monolithic alloy. They also found that such improvement in the mechanical properties was observed at both room and elevated temperatures up to 300˚C. They also showed that with increasing the volume fraction and/or reducing the size of Al_2O_3 nano-particulates increase both the tensile and yield strengths of the nanocomposites. While El-Mahallawi and Abdelkader (2012) studied the properties of A356 aluminum alloy incorporated with Al_2O_3 nano-particles. They showed that enhancement in the mechanical strength of the Al_2O_3 nano-dispersed alloys and increase in the elongation percentage supported by evidence of refined dendrite arms length, and inter-lamellar spacing were obtained. The properties of nano-sized Al_2O_3 particles reinforced 2024 aluminum matrix composites fabricated using conventional stir casting technique was studied by Su et al. (2012). They found that the ultimate tensile strength and yield strength of 1 wt.% nano-Al_2O_3/2024 composite were enhanced by 37% and 81%, respectively compared with the reference alloy.

The aim of this work was to study the effect of adding different percentages with different sizes of Al_2O_3 nano particles on the wear behavior of A356 alloy as well as to define the effect of hot deformation with different ratios on the wear behavior of Al_2O_3/A356 nano composite.

2. Experimental Work

The starting materials used in this work to prepare A356 matrix alloy were commercial purity aluminum, Al–10%Si master alloy and high purity magnesium. All starting materials were melted in an electric resistance furnace. After adjusting chemical composition, the molten A356 alloy was poured at temperature of 680 °C into the metallic mould with dimensions of 20x20x130 mm. The prepared A356 master alloy was analyzed using Optical Emission Spectrometer to determine the chemical composition as shown in Table 1.

Table 1. Chemical composition of prepared A356 Al alloy

Alloy type	Chemical composition, %						
	Si	Mn	Mg	Zn	Cu	Ni	Al
A356 Al alloy	6.67	0.209	0.45	0.092	0.20	0.070	Balance

The Al_2O_3/A356 nano-composites were prepared using graphite crucible which placed in the resistance furnaces. Stainless steel impeller with two blades equipped with electrical motor was used to stir the melt at rotating speed of 800 rpm.A digital thermometer with thermocouple type K was used to monitor and record the temperature of the melt. Before stirring, the specified amount of nano Al_2O_3 particles with specified particle size was wrapped with an aluminum foil and heated to 400°C for two hours. The preheated Al_2O_3 nano particles were added inside the vortex formed due to stirring. After completing the addition of nano Al_2O_3 particles, the stirring was stopped and the mixture of molten aluminum alloy with nano particles was poured into preheated medium carbon steel mould. The produced as-cast nano composites were cut and prepared for further investigation.

The compression apparatus type Instron (WDW - 200E) was used to deform the as-cast A356 alloy and Al_2O_3/nano-composite specimens. Cylindrical specimens with 10 mm in diameter and 20 mm in height were machined from the prepared as-cast A356 nano-composites. The specimens were heated to test temperature and held for 15 min. Hot deformations were carried out at the temperature of 250 °C and strain rate of $0.1 \ s^{-1}$ using hot deformation die designed for this purpose. Thermocouple type k was embedded in the mid-height of the samples which was used to monitor the actual temperature during testing. Different deformation ratios were achieved 30% and 40%. The deformation ratio is represented as $\Delta L/L_0$, where ΔL is the length of deformed sample and L_0 the length of sample before deformation.

Dry sliding wear tests were conducted in air at room temperature using a laboratory pin-on-disc wear apparatus. The pins, which are A356 alloy and nano Al_2O_3/A356 composites cylinders with dimensions of 10 mm in diameter and 20 mm in height, were ground with different SiC paper of (220, 320, 500, 800 and 1000) grit, polished with diamond paste, cleaned with acetone and then dried in hot air before test. The disc was made from M2 tool steel with a hardness of about 65 HRC. The loads used were 4.9, 9.8 and 14.7 N. The disc was always cleaned and polished periodically after each test.

3. Results and Discussion

Figure 1 shows the micrograph of as-cast A356 Al alloy which consists of primary α –Al phase (white regions) and Al-Si eutectic (dark regions).The eutectic phase appears as a continuous phase surrounding the α-Al dendrites. These phases were demonstrated using XRD as shown in figure 2.The Al_2O_3 nano particles that added to the matrix of A356 alloy presented individually and clustered mostly near and within the grain boundaries of α-Al phase as shown in Figure 3. This may be attributed to creation of what is called Al_2O_3 nano-particles enriched zone, which encapsulates nano Al_2O_3 particles.
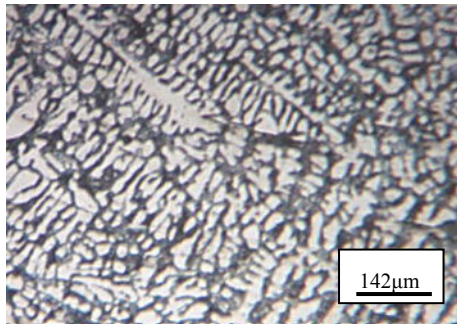
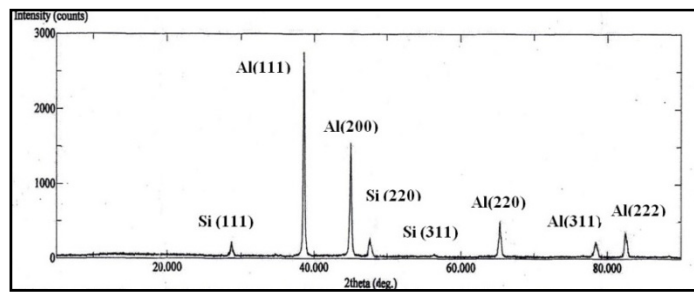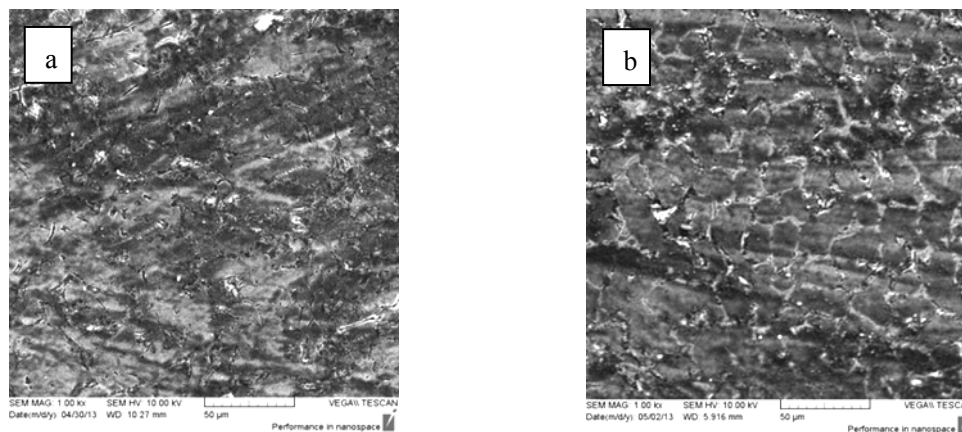Figure 1. The microstructure of A356 alloy   Figure 2. The XRD of A356 alloy

Figure 3. SEM image of nano Al_2O_3/A356 composites, (a) 1%Al_2O_3 (10 nm), (b) 2%Al_2O_3 (10 nm)

Figure 4 shows the relationship between the hardness values of the nano-composites with different weight percentages of Al_2O_3 nano-particles. It is obvious that the nano Al_2O_3/A356 composite exhibits higher hardness than the as-cast A356 alloy. The average hardness value of the nano-composites increases with increasing the weight percentage of the Al_2O_3 nano-particles. This may be due to the grain refinement and grain boundary suffers pinning. The average hardness of the nano-composites increased with increasing the hot deformation ratio and weight percentage of the Al_2O_3 nano-particles added. Furthermore, the hot deformed Al_2O_3/A356 nano composites containing 20 nm Al_2O_3 particles exhibited slightly higher average hardness when compared with the hot deformed one containing 10 nm Al_2O_3 particles.
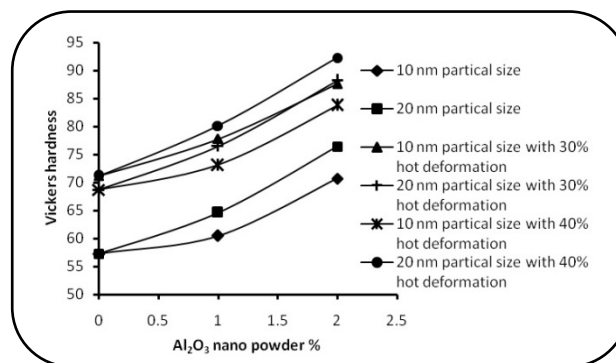
Figure 4. The relationship between hardness and nano Al_2O_3 percentage of hot deformed A356 alloy

The relationship between wear rate and applied loads of tested materials is presented in Figure 5. It is obvious from this figure that the wear rate decreased with increasing the percentage and size of nano Al_2O_3 particles.

Furthermore, with increasing applied load, wear rate increased regardless the reinforcement percentage and size. No transition of the wear regime could be recognized in the dry sliding of nano Al_2O_3/A356 composites on the steel counterface. This indicates that one wear regime took place according to the applied loads used. The wear regime is mixed between mild and sever one.

Two major wear mechanisms can be observed. These are oxidative and metallic wear. The percentage of each type depends on the reinforcement amount and size, and applied load used. Oxidative wear was observed at low applied loads in which aluminum oxide layer formed on both the wearing nano Al_2O_3/A356 composite surface and the counterface. The mechanism is concentrated on the oxidation of the pin surface asperities of the nano Al_2O_3/A356 composite firstly and secondly by the fracture and compaction of the generated oxidized wear debris into this film. On the other hand, metallic wear occurred and became predominant at high applied loads, which was characterized by plastic deformation and fracture. Furthermore, material transfer between nano Al_2O_3/A356 composite and counterface material with metallic wear debris generation was main features of this mechanism.

The decrease in wear rate with presence of nano Al_2O_3 particles, as shown in Figure 5, is most likely related to the role of these particles to prevent sever wear by protecting the soft matrix of α- aluminum phase and improving wear resistance. Therefore, wettability between nano Al_2O_3 particles and the matrix has crucial role on the enhancing wear resistance and also reflects the degree of bonding between them. If there is a good bonding, i.e. good wettability, the α-aluminum phase will worn away in the region that surround the nano Al_2O_3 particles. This means that all contact will be between the nano Al_2O_3 particles and the counterface material. The shear stress during sliding at the nano Al_2O_3 particles/A356 matrix may leads to decohesion of the nano Al_2O_3 particles which may change the wear rate according to the locations of decohesion of nano Al_2O_3 particles. Accordingly, the wear rate increases with increasing the locations of nano Al_2O_3 particles decohesion. From this, one can postulate that decrease in wear rate with increasing nano Al_2O_3 particles size is related to the well bond of nano Al_2O_3 particles with matrix. This depends on the surface area of nano Al_2O_3 particles where increasing the size of Al_2O_3 particles is associated with increasing surface area. This means that the bond area of nano Al_2O_3 with the matrix is greater for 20 nm compared with that for 10 nm.
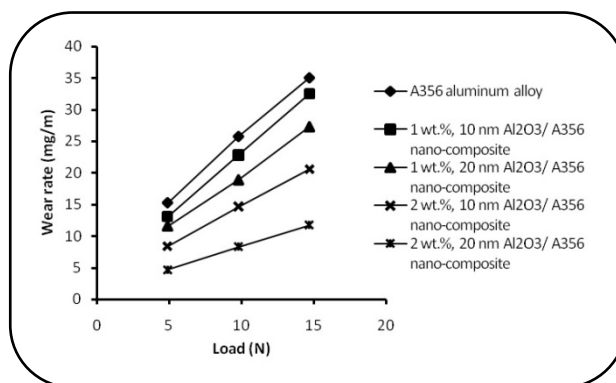

Figure 5. The relationship between wear rate and applied loads of nano Al_2O_3/A356 composites

The wear mechanism operating during dry sliding wear of nano Al_2O_3/A356 composites was determined using SEM. The predominant wear mechanism depends on the reinforced material characteristics, applied load and wear test conditions. In this work, all tests were performed under air atmosphere and at room temperature. SEM micrographs of worn surfaces of tested materials are presented in Figure 6. It shows grooves and scoring on the worn surface of tested materials. These grooves originate from the ploughing of wear test pin surface. The spacing between these grooves is not the same and its value depends on the tested material composition with constant of other wear test variables. While scoring marks may be due to the presence of Al_2O_3 particles within wear debris, wear debris are generated by fracture of pin surface. This debris may be accumulated in some of the adhesives wear grooves and distributed on the pin worn surface. It is clear from topographical features of worn surface that delamination wear is the predominant mechanism of sliding wear. Delamination wear theory is based on several steps which represented elsewhere (Clarke and Sarkar, 1981).

During dry sliding wear, transfer of material from pin surface to the counterface material surface has been observed. The magnitude of transferred material depends on the applied load. This was examined using naked eye inspection. In the other side, some transfer of material from counterface surface to the pin surface has been

taken place. This can be seen clearly by black spots on the pin surface as shown in Figure 6(d). Vencl et al. (2008) found that black spots represented an iron transferred from the counter body to the pin surface. They also found that minor extent of oxygen was also detected on the worn surface.
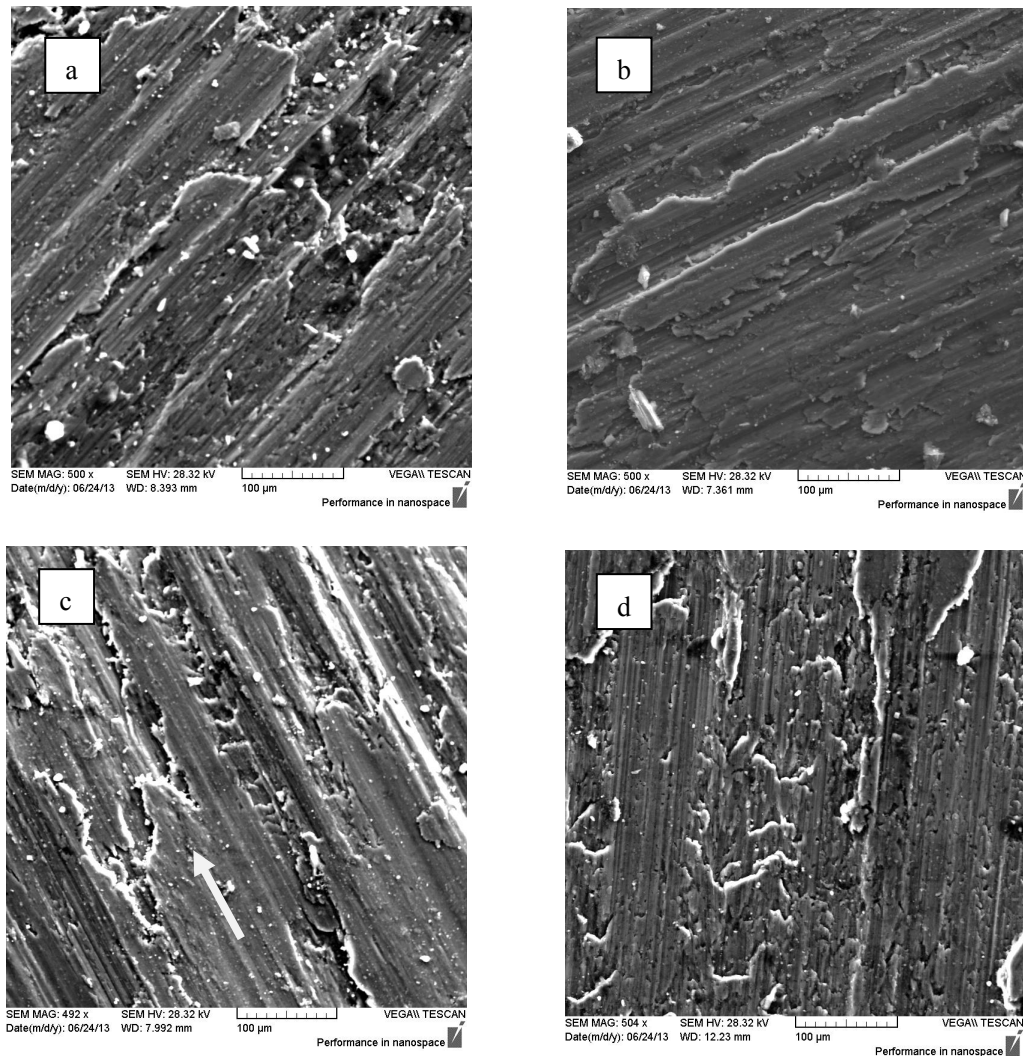

Figure 6. Secondary electron image of pin worn surface, a-A356 matrix alloy, b-1wt% 10 nm Al_2O_3/A356, c-2wt% 10 nm Al_2O_3/A356 and d-2wt% 20 nm Al_2O_3/A356

The effect of hot deformation with different percentage on the wear behavior of nano Al_2O_3/A356 composites are shown in Figs. 7 and 8 which represent the relationship between wear rate and applied loads. It is obvious from these figures that no differences were found in the wear behavior between hot deformed and non deformed nano Al_2O_3/A356 composites except in the magnitude of wear rate which depends on the applied loads. Hot deformation could increase the wear resistance of the nano Al_2O_3/A356 composites in comparison with non deformed one. Furthermore, increasing the hot deformation from 30% to 40% led to decrease the wear rate. This can be explained on the basis that with increasing hot deformation percentage, hardness increases with a magnitude depending on the percentage of nano Al_2O_3/A356 particles and size. The general relationship between hardness and wear resistance is linear (Bolton, 1998). Therefore, generally with increasing hardness value for a given material, wear rate will decrease, so that 40% hot deformed nano Al_2O_3/A356 composites have little wear rate compared with the 30% hot deformed and non deformed one. Furthermore, the presence of nano Al_2O_3 particles in the matrix withstands the applied loads as explained before. Therefore, these two factors have vital role in increasing the wear resistance of nano Al_2O_3/A356 composites with increasing hot deformation percentage.

The main wear mechanisms of hot deformed nano Al_2O_3/A356 composites are oxidative and metallic wear. One

wear regime can be clearly seen as depicted from Figs. 7 and 8. This wear regime is mixed between mild and sever wear. The same figures also show that hot deformed nano Al_2O_3/A356 composites have greater wear resistance compared with hot deformed A356 alloy. Furthermore, with increasing the size and percentage of Al_2O_3 nano particles wear rate will decrease.
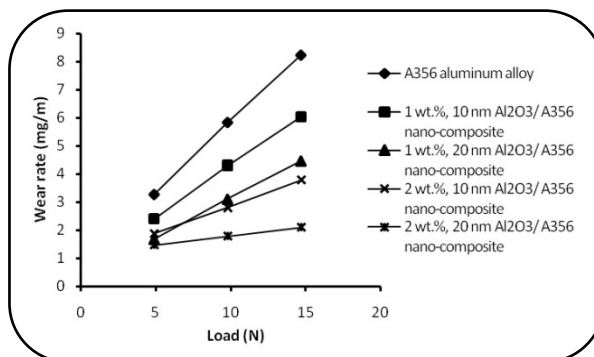

Figure 7. The relationship between wear rate and applied loads of 30% hot deformed nano Al_2O_3/A356 composites
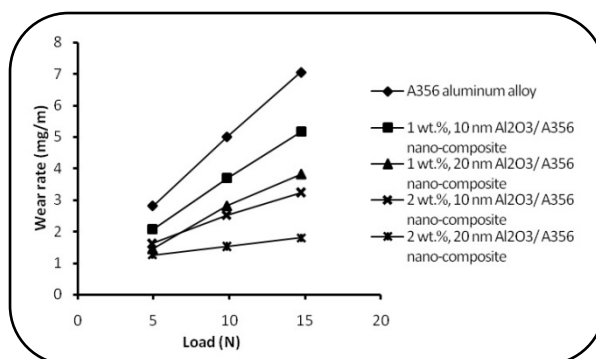

Figure 8. The relationship between wear rate and applied loads of 40% hot deformed nano Al_2O_3/A356 composites

The results of the worn surface study that we reported are mainly from SEM studies of the dry sliding of hot deformed nano Al_2O_3 /A356 composites with aid of the naked eye observation. Observations on the counterface surface are also reported. All adhesive wear experiments of hot deformed nano Al_2O_3 /A356 composites are carried out also at room temperature. It is clear from Figure 9, which represent the worn surface of tested materials with percentage of 30% hot deformation, that different wear mechanisms are contributed during dry sliding wear. Fine grooves can be seen in Figure 9(a) with some wear debris adhered on the worn surface. Deep grooves can be seen in Figure 9(b) which resulted from counterbody penetrates in to the pin surface causing plastic deformation. Furthermore, the initiation of roof tiles is seen to be within local areas.
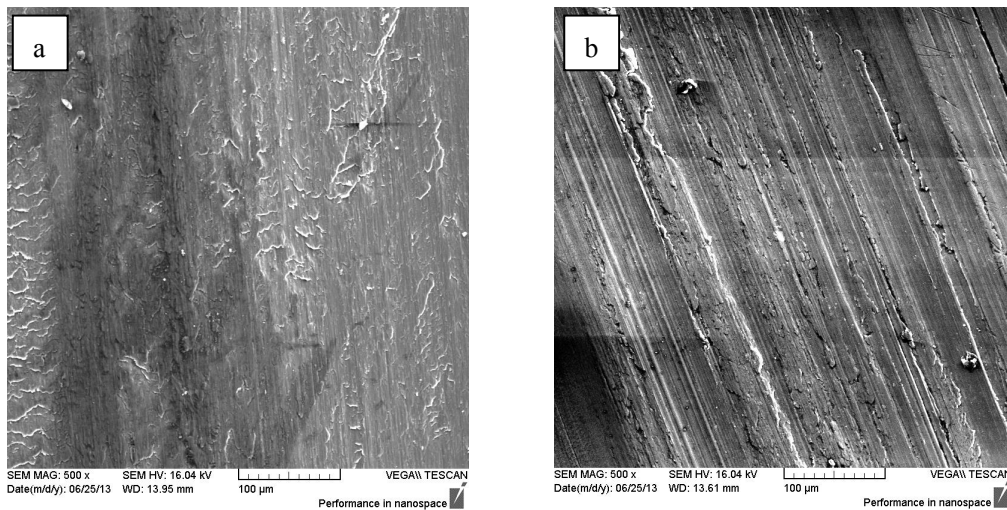
Figure 9. Secondary electron image of pin worn surface of 30% hot deformed test, a-2wt% 10 nm Al_2O_3/A356 and b-1wt% 20 nm Al_2O_3/A356

Adhesive delamination can be seen clearly in Figure 10(a). This mechanism is combined with plastic flow and adhesion effect. Small cracks can be observed on the worn surface which appears to be transverse to the sliding direction. From the nature of these small cracks, it is suggested that these cracks are the origin of delamination wear initiation. Shallow surface crater is apparent on the worn surface of 40% hot deformed nano Al_2O_3/A356 composites, as shown in Figure 10(b), which giving the appearance that the material had delaminated from it. Plastic flow and adhesion effects are also associated with this mechanism of material removal. This mechanism of material removal is explained elsewhere (Clarkr and Sarkar, 1981).

In the same manner as that for non deformed nano Al_2O_3/A356 composites, material transfer from the pin surface to the counterface surface has been taken place during dry sliding. These transferred materials roughen the counterface surface and therefore increases the wear rate with increasing applied loads. Furthermore, transferred material has significant role on determination the mechanism of material removal. It is appeared from the study that several mechanisms contributed to removal the pin surface material during adhesive wear. On other hand, the fractured surface, evident in the form of broken particles can also be seen on worn surface of hot deformed nano Al_2O_3/A356 composites.
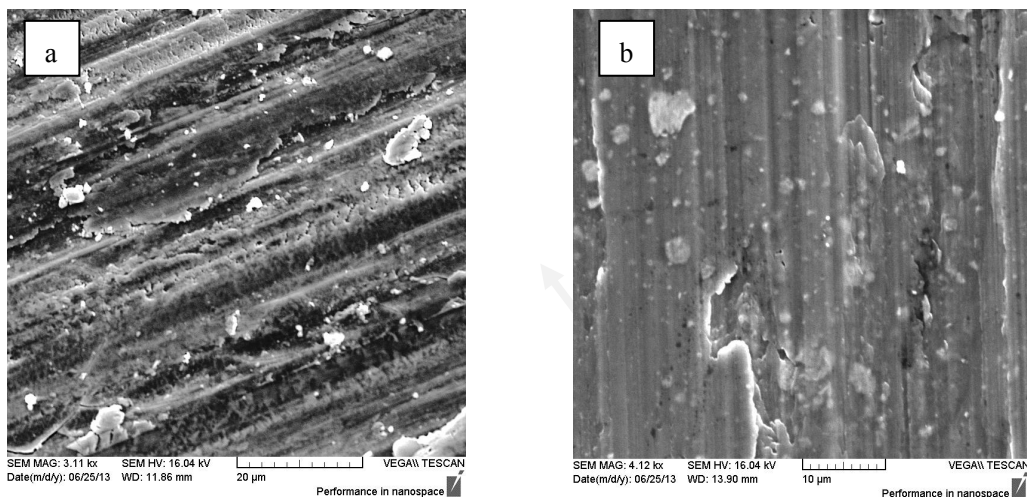

Figure 10. Secondary electron image of pin worn surface of 40% hot deformed test, a-2wt% 10 nm Al_2O_3/A356 and b-2wt% 20 nm Al_2O_3/A356

4. Conclusions

1-The average hardness value of the nano-composites increases with increasing the weight percentage of Al_2O_3 nano-particles.

2-The nano-composites containing 20 nm particles exhibited slightly higher hardness when compared with the Al_2O_3/A356 composites containing 10 nm Al_2O_3 particles after hot deformation.

3-The wear resistance of the Al_2O_3/A356 nano-composites was found to be considerably higher than that of the matrix alloy and it increases with increasing particle size and percentage.

4-The optimal results are achieved at the nano-composite containing 20 nm Al_2O_3.

5-The predominant wear mechanism was oxidative - metallic.

References

Bolton, W. (1994). Engineering Materials Technology, second ed., Butterworth – Heinemann, London.

Canyook, R., Petsut, S., Wisutmethangoon, S., Flemings, M. C., & Wannasin, J. (2010). Evolution of Microstructure in Semi-Solid Slurries of Rheocast Aluminum Alloy, Trans. *Nonferrous Met. Soc. China, 20*, 1649-1655.

Clarke, J., & Sarkar, A. D. (1981). Topographical Features Observed in a Scanning Electron Microscopy Study of Aluminum Alloys Surfaces in Sliding Wear. *Wear, 69*, 1-23.

El-Kady, E. Y., Mahmoud, T. S., & Sayed, M. A. (2011). Elevated Temperatures Tensile Characteristics of Cast A356/Al2O3 Nanocomposites Fabricated Using a Combination of Rheocasting and Squeeze Casting Techniques. *Mater. Sci. Applica., 2*, 390-398.

El-Mahallawi, I., & Abdelkader, H. (2012). Influence of Al_2O_3 Nano-Dispersions on Microstructure Features and Mechanical Properties of Cast and T6 Heat-Treated AlSi Hypoeutectic Alloys, *Mater. Sci. Eng. A, 556*, 76-87.

Saheb, N., Iqbal, Z., Khalil, A., Hakeem, A. S., Al Aqeeli, N., Laoui, T., Al-Qutub, A., & Kirchner, R. (2012). Spark Plasma Sintering of Metals and Metal Matrix Nano Composites: A Review. *J. Nanomater., 2012*, 1-13.

Su, H., Gao, W., Feng, Z., & Lu, Z. (2012). Processing, Microstructure and Tensile Properties of Nano-Sized Al_2O_3 Particle Reinforced Aluminum Matrix Composites. *Mater. Design, 36*, 590-596.

Vencl, A., Bobić, I., Jovanović, M. T., Babić, M., & Mitrović, S. (2008). Microstructural and Tribological Properties of A356 Al–Si Alloy Reinforced with Al_2O_3 Particles. *Tribol Lett, 32*, 159-170.

Zhou, Q., Zeng, L., DeCicco, M., Li, X., & Zhou, S. (2012). A Comparative Study on Clustering Indices for Distribution Uniformity of Nano-Particles in Metal Matrix Nanocomposites, *CIRP J. Manufact. Sci. Technol., 5*, 348-356.

Copyrights